nature genetics

Mutations in *TCF12*, encoding a basic helix-loop-helix partner of TWIST1, are a frequent cause of coronal craniosynostosis

Vikram P Sharma[1,2,20], Aimée L Fenwick[1,20], Mia S Brockop[3,4,20], Simon J McGowan[5], Jacqueline A C Goos[6,7], A Jeannette M Hoogeboom[8], Angela F Brady[9], Nu Owase Jeelani[10], Sally Ann Lynch[11], John B Mulliken[12], Dylan J Murray[13], Julie M Phipps[1], Elizabeth Sweeney[14], Susan E Tomkins[15], Louise C Wilson[16], Sophia Bennett[17], Richard J Cornall[17], John Broxholme[18], Alexander Kanapin[18], 500 Whole-Genome Sequences (WGS500) Consortium[19], David Johnson[2], Steven A Wall[2], Peter J van der Spek[7], Irene M J Mathijssen[6], Robert E Maxson[3,21], Stephen R F Twigg[1,20,21] & Andrew O M Wilkie[1,2,21]

Craniosynostosis, the premature fusion of the cranial sutures, is a heterogeneous disorder with a prevalence of ~1 in 2,200 (refs. 1,2). A specific genetic etiology can be identified in ~21% of cases[3], including mutations of *TWIST1*, which encodes a class II basic helix-loop-helix (bHLH) transcription factor, and causes Saethre-Chotzen syndrome, typically associated with coronal synostosis[4–6]. Using exome sequencing, we identified 38 heterozygous *TCF12* mutations in 347 samples from unrelated individuals with craniosynostosis. The mutations predominantly occurred in individuals with coronal synostosis and accounted for 32% and 10% of subjects with bilateral and unilateral pathology, respectively. *TCF12* encodes one of three class I E proteins that heterodimerize with class II bHLH proteins such as TWIST1. We show that TCF12 and TWIST1 act synergistically in a transactivation assay and that mice doubly heterozygous for loss-of-function mutations in *Tcf12* and *Twist1* have severe coronal synostosis. Hence, the dosage of TCF12-TWIST1 heterodimers is critical for normal coronal suture development.

Our exome sequencing approach focused on bilateral coronal craniosynostosis (**Fig. 1**) because of previous evidence that this pathological group is loaded with cases of monogenic etiology[3]. We examined the variant lists from the whole-exome data[7] of seven unrelated individuals with bilateral coronal synostosis, negative for previously described mutations[8], for genes showing nonsynonymous changes in two or more samples. Two samples had different heterozygous frameshift mutations in *TCF12* (encoding transcription factor 12; also known as HEB, HTF4 and ALF1)[9–11]; one (family 19) had a single-nucleotide deletion, and the other (family 30) had a four-nucleotide deletion (details in **Supplementary Table 1**). The mutations were confirmed by dideoxy sequencing of the original DNA samples (primary sequence results for all families are shown in **Supplementary Fig. 1**). In addition, a text search of the exome sequence data identified a new c.1468–20>A variant in *TCF12* in a third sample (family 22), located 20 nucleotides upstream of the start of exon 17. This variant was predicted to generate a cryptic splice acceptor site that was confirmed experimentally (**Supplementary Fig. 2a**). Thus, we had identified different heterozygous disruptive mutations of *TCF12* in three of seven samples from individuals with bilateral coronal synostosis. We interrogated other exome or whole-genome sequencing projects on craniosynostosis that we were undertaking concurrently: this analysis identified additional *TCF12* mutations in two siblings with bilateral coronal synostosis and their clinically unaffected mother (family 20, which we had erroneously analyzed assuming recessive inheritance) and in two unrelated individuals (from families 11 and 16) with clinical diagnoses of Saethre-Chotzen syndrome who did not have identified mutations in the *TWIST1* gene[4–6].

[1]Clinical Genetics Group, Weatherall Institute of Molecular Medicine, University of Oxford, Oxford, UK. [2]Craniofacial Unit, Oxford University Hospitals National Health Service (NHS) Trust, Oxford, UK. [3]Department of Biochemistry and Molecular Biology, University of Southern California/Norris Cancer Center, Los Angeles, California, USA. [4]Université Paris–Sud, Orsay, France. [5]Computational Biology Research Group, Weatherall Institute of Molecular Medicine, University of Oxford, Oxford, UK. [6]Department of Plastic and Reconstructive Surgery, Erasmus Medical Center, University Medical Center Rotterdam, Rotterdam, The Netherlands. [7]Department of Bioinformatics, Erasmus Medical Center, University Medical Center Rotterdam, Rotterdam, The Netherlands. [8]Department of Clinical Genetics, Erasmus Medical Center, University Medical Center Rotterdam, Rotterdam, The Netherlands. [9]Kennedy Galton Centre, North West London Hospitals NHS Trust, London, UK. [10]Department of Neurosurgery, Great Ormond Street Hospital for Children NHS Trust, London, UK. [11]National Centre for Medical Genetics, Our Lady's Children's Hospital, Dublin, Ireland. [12]Department of Plastic and Oral Surgery, Children's Hospital, Boston, Massachusetts, USA. [13]National Paediatric Craniofacial Centre, Children's University Hospital, Dublin, Ireland. [14]Department of Clinical Genetics, Liverpool Women's NHS Foundation Trust, Liverpool, UK. [15]Clinical Genetics Department, Musgrove Park Hospital, Taunton, UK. [16]North East Thames Regional Genetics Service, Great Ormond Street Hospital for Children NHS Trust, London, UK. [17]Medical Research Council (MRC) Human Immunology Unit, Weatherall Institute of Molecular Medicine, University of Oxford, Oxford, UK. [18]Wellcome Trust Centre for Human Genetics, University of Oxford, Oxford, UK. [19]A list of members and affiliations is provided in the **Supplementary Note**. [20]These authors contributed equally to this work.[21]These authors jointly directed this work. Correspondence should be addressed to R.E.M. (robert.maxson@med.usc.edu) or A.O.M.W. (andrew.wilkie@imm.ox.ac.uk).

Received 4 September 2012; accepted 20 December 2012; published online 27 January 2013; doi:10.1038/ng.2531

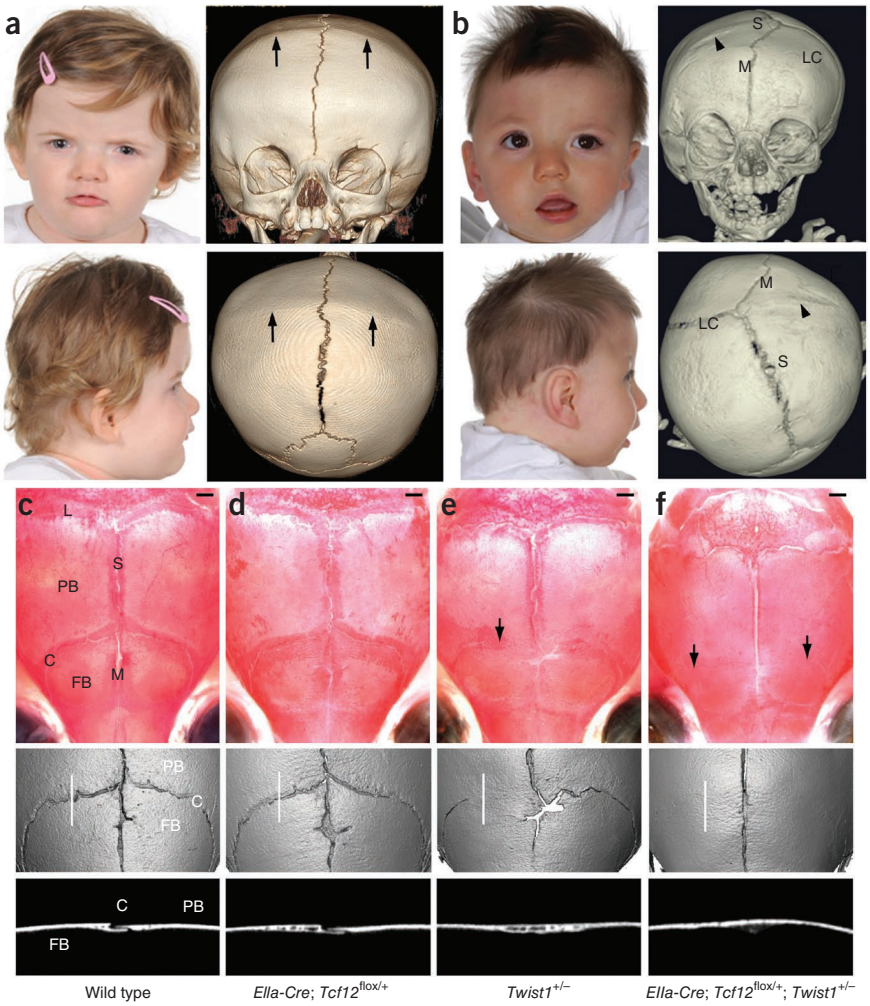

Figure 1 Phenotype associated with *TCF12* or *Tcf12* haploinsufficiency in humans and mice. (**a**,**b**) Clinical presentation of individuals with *TCF12* mutations, showing facial appearance (left) and computed tomography (CT) images of the head (right). Written permission was obtained to publish the clinical photographs. (**a**) Bilateral coronal synostosis in the proband from family 30: note the high forehead and brachycephaly at the age of 13 months. CT images at the age of 4 months show bilateral fusion of the coronal sutures associated with bony ridging (arrows). (**b**) Right unilateral coronal synostosis in the proband from family 35: at the age of 10 months, note the elevation of the right orbit and shifting of the midface and mandible to the left. CT images at the age of 4 months show complete fusion of the coronal suture on the right (arrowhead), an open coronal suture on the left (LC) and relative angulation of the metopic (M) and sagittal (S) sutures. (**c**–**f**) Severe bilateral coronal synostosis in *Ella-Cre*; *Tcf12*$^{flox/+}$; *Twist1*$^{+/-}$ combination mutants. Shown are representative images of postnatal day (P) 21 skulls stained with Alizarin Red S (top), three-dimensional μCT reconstructions (middle) and two-dimensional μCT images of sagittal slices (10 μm) through the coronal suture (bottom; the section planes are indicated by white lines in the three-dimensional images). Note the normal coronal sutures in the wild-type (**c**) and *Ella-Cre*; *Tcf12*$^{flox/+}$ (**d**) skulls, partial unilateral coronal synostosis in the *Twist1*$^{+/-}$ skull (**e**, arrow) and complete bilateral coronal synostosis in the *Ella-Cre*; *Tcf12*$^{flox/+}$; *Twist1*$^{+/-}$ skull (**f**, arrows). C, coronal suture; FB, frontal bone; L, lambdoid suture; PB, parietal bone. Scale bars, 1 mm.

To confirm these findings and explore the clinical consequences of *TCF12* mutations, we carried out dideoxy sequencing of *TCF12* in individuals with different types of craniosynostosis in whom mutations had not previously been identified. In the initial panel of 287 unrelated samples, we identified 18 with pathogenic mutations in *TCF12*; all mutation-positive individuals had coronal synostosis. To replicate our findings, we sequenced an independent Dutch cohort of 50 samples with coronal synostosis and identified 14 additional mutations in *TCF12*. Overall, we observed a strong bias for mutations in *TCF12* to occur in association with coronal synostosis (**Table 1**): 22 of 69 (32%) bilateral coronal and 14 of 141 (10%) unilateral coronal cases had mutations, but none of 93 cases with isolated metopic, sagittal or lambdoid synostosis had *TCF12* mutations ($P = 1 \times 10^{-6}$, Fisher's exact test). The remaining two cases positive for *TCF12* mutations had combinations of sagittal and either uni- or bilateral coronal synostosis, such that coronal synostosis was present in all 38 index subjects. In our extended Oxford birth cohort[3] with minimum 5-year follow-up (cases born in calendar years 1998–2006), we found *TCF12* mutations in 4 of 402 subjects (1.0%; 95% confidence interval of 0.3–2.5%). Hence, mutations in *TCF12* occur in a measurable fraction of craniosynostosis overall (**Supplementary Fig. 3**).

The mutations identified in *TCF12* comprise 14 nonsense, 15 frameshift, 7 splicing and 2 missense changes, suggesting a loss-of-function mechanism (**Fig. 2**). This is consistent with previous reports[12] of individuals with cytogenetically identified chromosome 15 deletions (predicted to include *TCF12* at 15q21.3) in whom craniosynostosis was present, although no whole-exon deletions of *TCF12* were detected in our subject panel using a multiplex ligation–dependent probe amplification (MLPA) assay. In cases with frameshift or splice-site mutations, analyses of mRNA extracted from various cell types showed lower expression of the mutant compared to the wild-type allele, consistent with nonsense-mediated mRNA decay (**Supplementary Fig. 2** and **Supplementary Table 2**). The mutations showed a clear enrichment in the 3′ half of *TCF12*, with all

Table 1 Identification of *TCF12* mutations in different categories of craniosynostosis

	Non-syndromic		Syndromic		Combined	
	Total	*TCF12* mutation positive	Total	*TCF12* mutation positive	Total	*TCF12* mutation positive
Metopic	32	0	14	0	46	0
Sagittal	32	0	7	0	39	0
Unilateral coronal	115	9	26	5	141	14
Bilateral coronal	28	5	41	17	69	22
Uni- or bilateral lambdoid	8	0	0	0	8	0
Multisuture	19	1	19	1	38	2
Sutures not specified	2	0	4	0	6	0
Combined	236	15	111	23	347	38

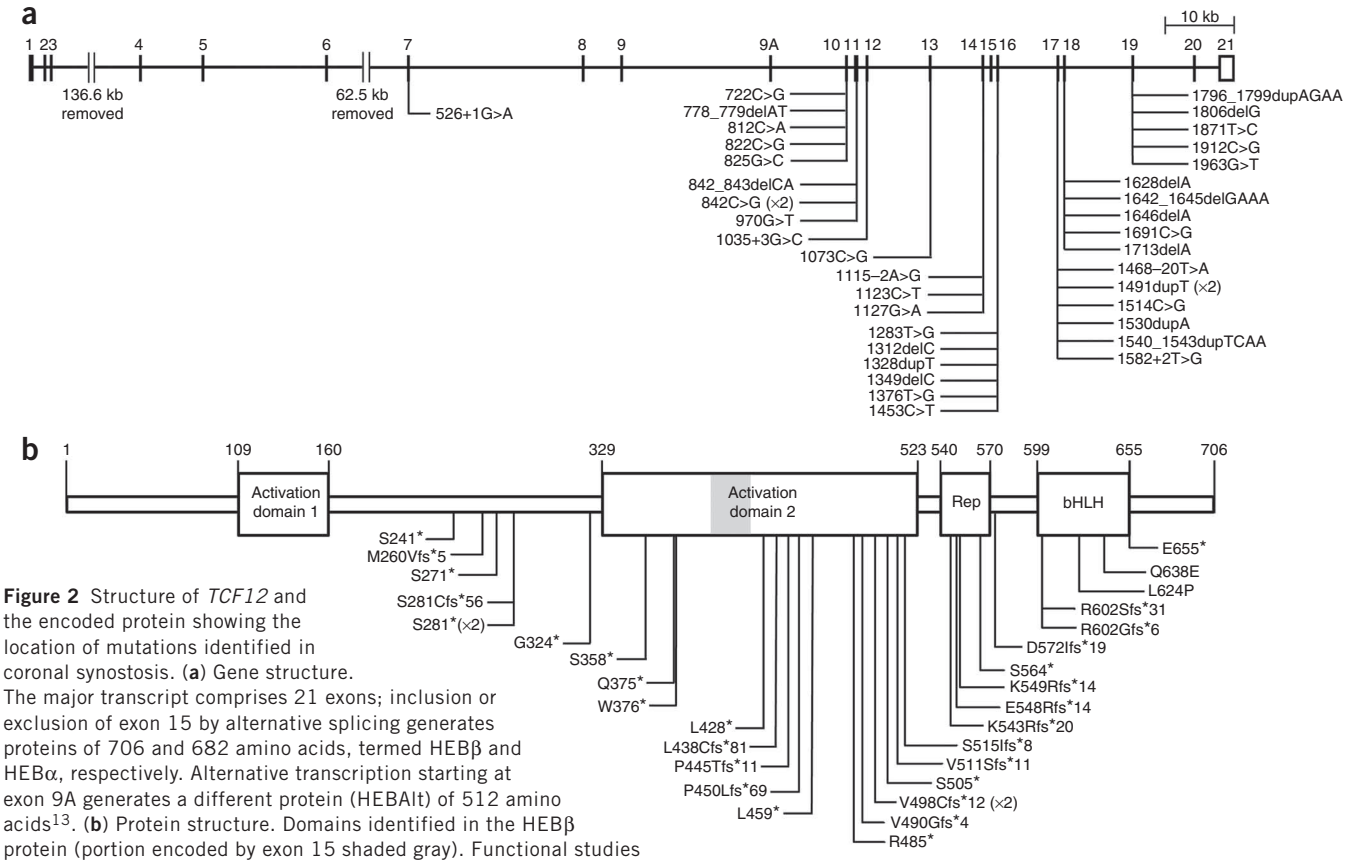

Figure 2 Structure of *TCF12* and the encoded protein showing the location of mutations identified in coronal synostosis. (**a**) Gene structure. The major transcript comprises 21 exons; inclusion or exclusion of exon 15 by alternative splicing generates proteins of 706 and 682 amino acids, termed HEBβ and HEBα, respectively. Alternative transcription starting at exon 9A generates a different protein (HEBAlt) of 512 amino acids[13]. (**b**) Protein structure. Domains identified in the HEBβ protein (portion encoded by exon 15 shaded gray). Functional studies previously defined activation domains 1 and 2 (ref. 24) and the rep domain[25]. Identical mutations identified in independent families are indicated (×2); note that mutations predicted to affect splicing are omitted from the protein schematic.

but one located between exons 10 and 19. The remaining mutation (c.526+1G>A), which caused skipping of exon 7 (**Supplementary Fig. 2d**), is specific to the longer *TCF12* transcript, as the alternative transcription start site[13] lies downstream of this position (exon 9A; **Fig. 2a**). The two missense mutations (encoding p.Leu624Pro and p.Gln638Glu substitutions) affect highly conserved residues of the bHLH domain required for dimerization (**Supplementary Fig. 4a**,**b**); mutations of other bHLH proteins often affect this region, with examples including alterations of the class I protein TCF4 (Pitt-Hopkins syndrome)[14] and class II protein TWIST1 (ref. 6). Using a transactivation assay with a reporter containing three E-boxes[15], we found that the combination of native TCF12 and TWIST1 proteins had a synergistic effect on activation relative to the activity of either protein individually, but this effect was 65–76% lower in the presence of the TCF12 missense mutations encoding p.Leu624Pro or p.Gln638Glu alterations (**Supplementary Fig. 4c).**

Of 36 families from which additional samples were available, the *TCF12* mutation was shown to have arisen *de novo* in 14 (**Supplementary Fig. 1** and **Supplementary Table 1**), providing further evidence that the *TCF12* mutations are causative of the coronal synostosis phenotype. In 23 of the families, cascade testing identified 34 additional mutation-positive individuals, only 16 of whom had craniosynostosis or other relevant clinical features, indicating substantial (53%) non-penetrance (**Supplementary Table 1**; see **Supplementary Fig. 5** for representative clinical photographs). There was no evidence to implicate somatic mosaicism in any of the non-penetrant cases, but preliminary analysis of haplotypes around *TCF12* (which resides in a region of strong linkage disequilibrium) suggested that the allelic backgrounds of both non-mutant and mutant copies of *TCF12* contribute to variability in the phenotype (data not shown). Of 14 mutation-positive relatives diagnosed with craniosynostosis involving specific sutures, 12 had coronal synostosis, and 2 had sagittal synostosis.

The clinical features associated with *TCF12*-related craniosynostosis are detailed (**Supplementary Table 3**), and representative subjects with bilateral coronal synostosis (**Fig. 1a**) or unilateral coronal synostosis (**Fig. 1b**) are shown. In 15 probands (39%), a genetic cause was suspected because of a positive family history. In another seven probands (18%), clinical features (including dysmorphic appearance of the face and external ears and minor limb anomalies) were suggestive of Saethre-Chotzen syndrome, which had been excluded by negative *TWIST1* mutation testing. The remaining subjects (16/38 = 42%) presented sporadically with apparently non-syndromic synostosis (**Supplementary Table 1**). No genotype-phenotype correlation was detected. For affected individuals recruited at Oxford, we compared the surgical trajectory[3] of *TCF12*-positive individuals with those of individuals falling into other clinical and genetic categories. The individuals with *TCF12* mutations had a more benign course compared with individuals with either p.Pro250Arg FGFR3 or TWIST1 alterations (**Supplementary Fig. 6**), and no individuals positive for *TCF12* mutations were documented to have an interval onset of raised intracranial pressure after their initial surgical procedure(s). Most individuals had normal developmental attainment, but ten (14%) had developmental delay or learning disability, which in two cases was associated with autism (clinical features are summarized in **Supplementary Table 4).** Previous genetic data derived from homozygous mutant mice identified key roles for the orthologous

Tcf12 gene in the development of the immune system[13,16], but we found no history of infection susceptibility in individuals heterozygous for *TCF12* mutations, and there was no detectable reduction in monocyte, natural killer (NK), T-cell or B-cell subsets or lower amounts of immunoglobulin in 11 mutation-positive individuals.

Supporting our transactivation data (**Supplementary Fig. 4**), it was previously reported that TCF12 forms heterodimers with TWIST1 (ref. 17) and that *TWIST1* haploinsufficiency causes Saethre-Chotzen syndrome[4–6]. Our observation that haploinsufficiency of *TCF12* in humans leads specifically to coronal synostosis suggests that the total quantity of TCF12-TWIST1 heterodimers is a critical factor in coronal suture development. To test this hypothesis, we compared the phenotypes of the previously constructed individual heterozygous null mutant mice (*EIIa-Cre*; *Tcf12*$^{flox/+}$ and *Twist1*$^{+/-}$)[16,18,19] to that of the compound heterozygotes (*EIIa-Cre*; *Tcf12*$^{flox/+}$; *Twist1*$^{+/-}$). At 3 weeks of age, the *EIIa-Cre*; *Tcf12*$^{flox/+}$ animals ($n = 14$) had normal coronal sutures, indicating that the coronal suture is less sensitive to Tcf12 dosage in mice than in humans (**Fig. 1c**,**d**); *Twist1*$^{+/-}$ mice ($n = 4$) showed variable coronal synostosis, as previously reported (**Fig. 1e**)[5,20]. However, the *EIIa-Cre*; *Tcf12*$^{flox/+}$; *Twist1*$^{+/-}$ compound heterozygotes ($n = 6$), which were born at a frequency close to the expected Mendelian ratio (25%), consistently showed severe coronal synostosis (**Fig. 1f**).

The discovery that haploinsufficiency of *TCF12* causes coronal synostosis in humans and that severe bilateral coronal synostosis occurs in mice with 50% of the wild-type dosage of both the *Tcf12* and *Twist1* genes highlights the key role of TCF12 acting with TWIST1, probably as a heterodimeric complex, in the normal development of the coronal sutures. The TCF12-TWIST1 heterodimer is likely to regulate specification of the boundary between the neural crest and cephalic mesoderm[20,21] and/or inhibit osteogenic differentiation via actions on RUNX2 (ref. 22) and bone morphogenetic protein[23] or fibroblast growth factor receptor[17] signaling.

URLs. ANNOVAR, http://www.biobase-international.com/product/annovar; GBrowse2, http://gmod.org/wiki/GBrowse; MRC-Holland, http://www.mrc-holland.com/; PolyPhen-2 http://genetics.bwh.harvard.edu/pph2; SAMtools, http://samtools.sourceforge.net.

METHODS

Methods and any associated references are available in the online version of the paper.

Accession codes. All cDNA numbering of *TCF12* follows NCBI reference NM_207037.1, starting with A of the ATG initiation codon (+1). We used NM_207040.1 to design primers to the alternatively spliced first exon (9A). The genomic reference sequence is available under accession NC_000015.9.

Note: Supplementary information is available in the online version of the paper.

ACKNOWLEDGMENTS

We thank all the families for their participation, S. Butler for cell culture, J. Frankland and T. Rostron for DNA sequencing, S. Knight for coordinating array–comparative genomic hybridization (aCGH), L. Gregory and the High-Throughput Genomics core at the Wellcome Trust Centre for Human Genetics for exome sequencing, R. Evans for review of anesthetic records, W. Baggley for clinical photography, A. van den Ouweland for genetic testing, E.-M. Füchtbauer (Aarhus University) for constructs and Y. Zhuang (Duke University) for the gift of the *Tcf12*^{flox} mutant. This work was funded by the National Institute for Health Research (NIHR) Biomedical Research Centre Oxford (V.P.S. and R.J.C.), the Oxford University Clinical Academic Graduate School and the Oxfordshire Health Services Research Committee (V.P.S.), the Oxford Craniofacial Unit Charitable Fund (V.P.S.), the Thames Valley Comprehensive Local Research Network (J.M.P.), The Dutch Center for Translational Molecular Medicine (P.J.v.d.S.), the Carolien Bijl Foundation (J.A.C.G.), the US National Institutes of Health (NIH; R01DE016320 and R01DE019650 to R.E.M.) and the Wellcome Trust (093329 to S.R.F.T. and A.O.M.W.).

AUTHOR CONTRIBUTIONS

S.R.F.T., R.E.M. and A.O.M.W. conceived the project. V.P.S., A.L.F., M.S.B. and S.R.F.T. performed experimental analyses. S.B. and R.J.C. performed immune function tests. S.J.M., J.B., A.K. and WGS500 coordinated or performed bioinformatics analyses. V.P.S., J.A.C.G., A.J.M.H., A.F.B., N.O.J., S.A.L., J.B.M., D.J.M., J.M.P., E.S., S.E.T., L.C.W., D.J., S.A.W., P.J.v.d.S., I.M.J.M. and A.O.M.W. recruited samples from subjects and collected clinical information. V.P.S., A.L.F., R.E.M., S.R.F.T. and A.O.M.W. drafted the manuscript.

COMPETING FINANCIAL INTERESTS

The authors declare no competing financial interests.

Published online at http://www.nature.com/doifinder/10.1038/ng.2531.
Reprints and permissions information is available online at http://www.nature.com/reprints/index.html.

1. Lajeunie, E., Le Merrer, M., Bonaïti-Pellie, C., Marchac, D. & Renier, D. Genetic study of nonsyndromic coronal craniosynostosis. *Am. J. Med. Genet.* **55**, 500–504 (1995).
2. Boulet, S.L., Rasmussen, S.A. & Honein, M.A. A population-based study of craniosynostosis in metropolitan Atlanta, 1989–2003. *Am. J. Med. Genet.* **146A**, 984–991 (2008).
3. Wilkie, A.O.M. *et al.* Prevalence and complications of single-gene and chromosomal disorders in craniosynostosis. *Pediatrics* **126**, e391–e400 (2010).
4. Howard, T.D. *et al.* Mutations in *TWIST*, a basic helix-loop-helix transcription factor, in Saethre-Chotzen syndrome. *Nat. Genet.* **15**, 36–41 (1997).
5. El Ghouzzi, V. *et al.* Mutations of the *TWIST* gene in the Saethre-Chotzen syndrome. *Nat. Genet.* **15**, 42–46 (1997).
6. Jabs, E.W. *TWIST* and the Saethre-Chotzen syndrome. in *Inborn Errors of Development. The Molecular Basis of Clinical Disorders of Morphogenesis*, 2nd edn (eds. Epstein, C.J., Erickson, R.P. & Wynshaw-Boris, A.) 474–481 (Oxford University Press, Oxford, 2008).
7. Ng, S.B. *et al.* Exome sequencing identifies the cause of a mendelian disorder. *Nat. Genet.* **42**, 30–35 (2010).
8. Johnson, D. & Wilkie, A.O.M. Craniosynostosis. *Eur. J. Hum. Genet.* **19**, 369–376 (2011).
9. Hu, J.S., Olson, E.N. & Kingston, R.E. HEB, a helix-loop-helix protein related to E2A and ITF2, that can modulate the DNA-binding ability of myogenic regulatory factors. *Mol. Cell Biol.* **12**, 1031–1042 (1992).
10. Nielsen, A.L., Pallisgaard, N., Pedersen, F.S. & Jørgensen, P. Murine helix-loop-helix transcriptional activator proteins binding to the E-box motif of the Akv murine leukemia-virus enhancer identified by cDNA cloning. *Mol. Cell Biol.* **12**, 3449–3459 (1992).
11. Gan, T.-I. Genomic organization of human *TCF12* gene and spliced mRNA variants producing isoforms of transcription factor HTF4. *Cytogenet. Genome Res.* **98**, 245–248 (2002).
12. Hiraki, Y. *et al.* Craniosynostosis in a patient with a *de novo* 15q15-q22 deletion. *Am. J. Med. Genet.* **146A**, 1462–1465 (2008).
13. Wang, D. *et al.* The basic helix-loop-helix transcription factor HEBAlt is expressed in pro-T cells and enhances the generation of T cell precursors. *J. Immunol.* **177**, 109–119 (2006).
14. Whalen, S. *et al.* Novel comprehensive diagnostic strategy in Pitt-Hopkins syndrome: clinical score and further delineation of the *TCF4* mutational spectrum. *Hum. Mutat.* **33**, 64–72 (2012).
15. Laursen, K.B., Mielke, E., Iannaccone, P. & Fuchtbauer, E.M. Mechanism of transcriptional activation by the proto-oncogene *Twist1*. *J. Biol. Chem.* **282**, 34623–34633 (2007).
16. Wojciechowski, J., Lai, A., Kondo, M. & Zhuang, Y. E2A and HEB are required to block thymocyte proliferation prior to pre-TCR expression. *J. Immunol.* **178**, 5717–5726 (2007).
17. Connerney, J. *et al.* Twist1 dimer selection regulates cranial suture patterning and fusion. *Dev. Dyn.* **235**, 1345–1357 (2006).
18. Lakso, M. *et al.* Efficient *in vivo* manipulation of mouse genomic sequences at the zygote stage. *Proc. Natl. Acad. Sci. USA* **93**, 5860–5865 (1996).
19. Chen, Z.F. & Behringer, R.R. *twist* is required in head mesenchyme for cranial neural tube morphogenesis. *Genes Dev.* **9**, 686–699 (1995).
20. Merrill, A.E. *et al.* Cell mixing at a neural crest–mesoderm boundary and deficient ephrin-Eph signaling in the pathogenesis of craniosynostosis. *Hum. Mol. Genet.* **15**, 1319–1328 (2006).
21. Chai, Y. & Maxson, R.E. Jr. Recent advances in craniofacial morphogenesis. *Dev. Dyn.* **235**, 2353–2375 (2006).
22. Bialek, P. *et al.* A Twist code determines the onset of osteoblast differentiation. *Dev. Cell* **6**, 423–435 (2004).
23. Hayashi, M. *et al.* Comparative roles of Twist-1 and Id1 in transcriptional regulation by BMP signaling. *J. Cell Sci.* **120**, 1350–1357 (2007).
24. Aronheim, A., Shiran, R., Rosen, A. & Walker, M.D. The *E2A* gene-product contains two separable and functionally distinct transcription activation domains. *Proc. Natl. Acad. Sci. USA* **90**, 8063–8067 (1993).
25. Markus, M., Du, Z.M. & Benezra, R. Enhancer-specific modulation of E protein activity. *J. Biol. Chem.* **277**, 6469–6477 (2002).

ONLINE METHODS

Samples. The clinical studies were approved by Oxfordshire Research Ethics Committee B (reference C02.143), Riverside Research Ethics Committee (reference 09/H0706/20) and the Medical Ethical Committee of the Erasmus University Medical Center Rotterdam (MEC-2012-140). Written informed consent to obtain samples for genetics research was obtained from each child's parent or guardian. The clinical diagnosis of craniosynostosis was confirmed by CT scan, and evidence of associated syndromic features was sought by clinical examination. Venous blood was obtained for DNA and RNA extraction (collected into PAXgene Blood RNA tubes (Qiagen) for the latter procedure). Fibroblast cultures were established from skin biopsies obtained from the scalp incision at the time of surgical intervention. When clinically indicated, samples were tested for mutation hotspots in *FGFR2*, *FGFR3* and *TWIST1* (ref. 8), and significant chromosome aneuploidy was investigated using aCGH; samples with identified mutations known to cause craniosynostosis were excluded. Seven samples from unrelated individuals with bilateral coronal synostosis were chosen for exome sequencing. These comprised five subjects who were clinically non-syndromic with negative family history, one subject who was clinically non-syndromic but reported to have two children with coronal synostosis and one subject who was the only individual in the family affected with craniosynostosis but who had short thumbs that were also present in several additional family members from the two previous generations.

Exome sequencing. We used an Agilent SureSelect Human All Exon Kit (v.2; 44 Mb) to capture exonic DNA from a library prepared from 3 µg of each proband's genomic DNA (extracted from whole blood). The enriched DNA was sequenced on an Illumina Genome Analyzer IIx platform with 51-bp paired-end reads. We generated between 3.98 and 4.56 Gb of sequence for each sample that, after mapping with Novoalign (Novocraft Technologies) to the hg19 genome and removal of artifacts using custom Perl scripts, resulted in an average coverage of exons of between 33- and 44-fold. Variants were called using SAMtools and annotated using ANNOVAR and PolyPhen-2. We removed all variants annotated in dbSNP132 and manually examined the gene lists for overlaps of two or more variants. Sequence data were visualized using GBrowse2.

Analysis of *TCF12*. After the identification of candidate *TCF12* mutations in the exome sequence, we confirmed and extended this analysis by direct sequencing of genomic PCR amplification products, MLPA and analysis of cDNA products. Details of the oligonucleotides and experimental conditions are provided in **Supplementary Table 5**. Our initial screening panel mostly comprised samples recruited in Oxford[3] and other craniofacial units within the UK, and the replication panel comprised samples obtained in Rotterdam, The Netherlands. PCR amplification was performed in a volume of 20 µl, containing 15 mM Tris-HCl (pH 8.0), 50 mM KCl, 2.5 mM $MgCl_2$, 100 µM each dNTP, 0.4 µM primers and 0.5 units of Amplitaq Gold polymerase (Applied Biosystems), with or without 10% DMSO, as indicated. Cycling conditions consisted of an 8-min denaturation step at 94 °C, followed by 35 cycles of 94 °C for 30 s, annealing at 65 °C (unless otherwise indicated in **Supplementary Table 5**) for 30 s and extension at 72 °C for 30 s, with a final extension at 72 °C for 10 min. Amplification products were sequenced using the BigDye Terminator v3.1 cycle sequencer system (Applied Biosystems). All mutations were reconfirmed, either by restriction digestion of 5 µl of PCR product or by repeat dideoxy sequencing of an independent PCR product. In addition to the mutations listed in **Supplementary Table 1**, we identified two previously unreported variants in single individuals that are currently of uncertain pathogenic significance, c.630T>G (p.Ser210Arg) and c.982A>G (p.Asn328Asp).

Copy-number variation was analyzed by MLPA performed using synthetic oligonucleotide probes designed to *TCF12* according to protocols available from MRC-Holland. Fragments were analyzed by capillary electrophoresis using an ABI 3130 containing POP-7 polymer. Peaks were visualized using Gene Mapper v3.7 (Applied Biosystems). Normal MLPA results were obtained in 226 craniosynostosis samples negative for intragenic *TCF12* mutations. For studies of splicing and mRNA stability, RNA was extracted from whole blood and fibroblasts using TRIzol reagent. cDNA was synthesized using the Fermentas RevertAid First-Strand Synthesis kit with random hexamer primers according to the manufacturer's instructions. The microsatellites used to confirm sample relationships were *D3S1311*, *D4S403*, *D5S2027*, *D6S1610*, *D7S519*, *D9S158*, *D10S548*, *D11S898*, *D13S1265*, *D14S280*, *D16S415* and *D18S474*.

Immune function tests. Peripheral blood mononuclear cells (PBMCs) were isolated from whole blood by density gradient centrifugation in cell separation tubes (Sigma), washed three times in sterile PBS and rested overnight in RPMI 1640 medium supplemented with 10% FCS, 1% L-glutamine, 1% penicillin-streptomycin solution and 50 µM β-mercaptoethanol (all from Sigma) and 1% HEPES buffer (GibcoBRL). Monocytes, NK cells and naive, effector and memory T- and B-cell subsets were enumerated by flow cytometry of PBMCs stained with human-specific antibodies against CD3, CD4, CD19, CD14, CCR7, CD45RO, CD62L, CD16, CD56, CD25, IgD, IgM, CD10 and CD27 (**Supplementary Table 6**). Total IgM, IgA and IgG antibody titers were measured by ELISA.

Transactivation analysis of missense mutations. We obtained a full-length *TCF12* cDNA clone (pCMV6-XL5, encoding HEBβ) from OriGene and synthesized the *TWIST1* clone (pCMV-Twist) in house. The pCaSpeR-*Tinman*::*lacZ* (pTinE1/E2/E3) construct (containing three *Tinman* E-boxes comprising two 5′-CATGTG-3′ and one 5′-CATATG-3′) was used as a bHLH protein-responsive reporter, and placZ (containing no E-boxes) was used as a control (both constructs were gifts from E.-M. Füchtbauer)[15]. PCR mutagenesis was used to introduce the c.1871T>C and c.1912 C>G mutations into the *TCF12* cDNA using the primers indicated in **Supplementary Table 5**; mutated cDNAs were fully verified by sequencing.

The HT1080 human cell line was cultured in high-glucose DMEM (Invitrogen) supplemented with 10% FCS. Cells were transfected in triplicate with 1 µg of reporter plasmid, 1 µg each of *TWIST1* and *TCF12* constructs or the corresponding empty expression vectors using Promega FuGENE 6 transfection reagent according to the manufacturer's protocols. Transfections were carried out when cells were ~50% confluent in 6-well plates. Cells were harvested after 48 h, and β-galactosidase assays were performed in triplicate on 5 µl of cellular extract using the Galacto-Star system (Applied Biosystems). The missense mutations were modeled in Protein Workshop onto the structure of mouse E47/NeuroD1 (Protein Data Bank (PDB) accession 2QL2)[26].

Analysis of mouse mutants. The mouse mutants analyzed were *Tcf12*^{flox} (obtained on a mixed C57BL/6/129 background as a gift of Y. Zhuang)[16], *EIIa-Cre* (purchased from The Jackson Laboratory (B6.FVB-Tg(EIIa-cre) C5379Lmgd/J)[18] and *Twist1* (C57BL/6 background)[19]. The *EIIa-Cre* transgene was detected using primers Cre-F and Cre-R (**Supplementary Table 5**); *Tcf12*^{flox} and *Twist1* were genotyped as described[16,19]. Heads of P21 mice were skinned and stained for mineralized bone with Alizarin Red S (80 mg/l in 1% KOH) for 3 d. Skulls were then cleared and stored in 100% glycerol. P21 mouse skulls were scanned using a µCT system (SCANCO µCT 50, Scanco Medical AG) and analyzed using Amira software (Visage Imaging). All scans were conducted at an energy setting of 70 kVp, current intensity of 200 µA, integration time of 500 ms/projection, 0.24 degree rotational step (DRS) and a field of view (FOV) of 15.1 mm. Scans were performed at a 10-µm isotropic resolution.

26. Longo, A., Guanga, G.P. & Rose, R.B. Crystal structure of E47-NeuroD1/β2 bHLH domain-DNA complex: heterodimer selectivity and DNA recognition. *Biochemistry* **47**, 218–229 (2008).

doi:10.1038/ng.2531